Bulgarian Chemical Communications, Volume 47, Special Issue D, (pp. 179 – 186) 2015

Optimization electrophotocatalytic removal of acid red 18 from drinking water by the Taguchi model

Kashi Giti[1*], Jaberzadee Narges[2]

[1]*Department of Environmental Health, School of Health, Islamic Azad University Tehran Medical Sciences Branch, Tehran, Iran*

[2]*Department of Natural Sources Engineering, Environmental Pollution, Department of Environmental, Islamic Azad University, Damavand Pardice Science and Research Branch, Damavand, Iran*

Received June 26, 2015, Revised September 10, 2015

The aim of this applied-analytical research was to investigate acid red18(AR18)removal from water by a batch EPC reactor using zinc oxide (ZnO) nanoparticles immobilized on a zinc(Zn) sheet-copper electrode and an emitting dynode(LED)ultraviolet-A (UV-A) lamp. Various operating variables were tested; these include current density, initial concentration of AR 18, lamp intensity, concentration of ZnO nanoparticles, pH and radiation time. To prepare the ZnO films on the Zn electrode dry methods were used. The studied variables were pH(4-10), AR 18 concentration (100-300 mg L^{-1}), lamp intensity(120-360 mW cm^{-2}), radiation time(0-45 min), concentration of zinc oxide nanoparticles(1.5-4.5 mg cm^{-2}) and current density(3-9 mA cm^{-2}). The AR 18 concentration was measured by a spectrophotometer. The optimal removal(0) was obtained at pH 4, a radiation time of 30 minutes, 3 mg cm^{-2} of ZnO nanoparticles concentration, lamp intensity of 360 mW cm^{-2} and a current density of 9 mA cm^{-2}. The AR 18 degradation followed a first order reaction. The results of AR 18 removal efficiency via the Taguchi model indicated that the concentration was the most important variable. The rate of degradation decreased at higher concentrations. Thus, batch experiments showed that the EPC reactor can be considered a promising technology for treating AR 18-polluted water.

Key words: Acid red 18 (AR 18), Drinking water, Electrophotocatalytic, Taguchi model, Zinc oxide.

INTRODUCTION

We deal with a variety of chemical materials in the textile effluent such as enzymes, detergents, dyes, sodas, salts and acids [1]. Annual azo dyes (-N=N-) production in the world during 2010 is estimated to be about 350000 tons, including red, yellow, orange, blue, black, green and violet [2]. The characteristics of acid red 18 (AR 18), $C_{20}H_{11}N_2Na_3O_{10}S$, is a low lethal dose (8000 mg kg^{-1} bw in rat fed). AR 18 is approved for use as a food colorant and as a direct dye in semi-permanent hair dye. Azo dyes may be due to their toxicity a source of a potential danger to both human health and the environment [3]. The textile industry in Iran has been situated mainly in Yazd, Kashan and Mazandran states. The increase in AR 18 levels in the groundwater in the country of Iran has been mainly attributed to the discharge of dye effluent. The national emission standard for discharging into a surface water source has been promulgated as 75 TCU. A wide range of traditional methods are used for the treatment of AR 18-contaminated water including adsorption, chemical precipitation and reverse osmosis [4]. In recent years, advanced oxidation processes (AOPs) such as electrophotocatalytic (EPC) are applied to treat the dye-contaminated water [5]. The presence of a catalyst in the electrical field or combined and direct photoelectrochemical application increases the treatment efficiency with lower energy consumption [6]. This process is a coupling of electrochemistry with heterogeneous photo-catalysis to avoid photohole/photoelectron recombination [7]. The advantages of a thin layer electrophotocatalyst stabilized on a metal surface are; more homogeneous UV radiation of the catalyst and avoiding filtration [8]. Effective factors for the optimal performance of a thin layer electrophotocatalyst stabilized on a metal surface are: the catalyst gap bond, layer thickness, light intensity, oxygen and the presence of particles [9]. In this study the coupling of a light emitting dynode (LED) UV-A lamp and immobilized zinc oxide (ZnO) semiconductor on a zinc (Zn) electrode have introduced a new method to meet the efficient decay of AR 18. The aim of this study is the removal AR 18, an azo dye which is considered a dye stable to ultraviolet and visible light irradiation, from drinking water using a thin layer of photocatalytic ZnO nanoparticles stabilized on Zn.

To whom all correspondence should be sent:
E-mail: g.kashi11@yahoo.com

The studied variables are pH, the concentration of AR 18, the lamp intensity, the radiation time, the concentration of zinc oxide nanoparticles, and the current density.

EXPERIMENTAL

Materials

The ZnO nanoparticles with a special area of 50 m^2 g^{-1} and particle size of 20 nm were supplied by Amohr Co. (Germany). Sulphuric acid, AR 18, and sodium hydroxide were purchased from Merck Co. (Germany). Sulphuric acid and sodium hydroxide (1 N) were applied for pH adjustment.

Preparation of ZnO nanoparticles

5 grams of ZnO nanoparticles were placed into 100 ml of distilled water. To improve the dispersion of ZnO, the suspension was mixed with a magnetic stirrer for 30 min and then sonicated in an ultrasonic bath (MATR.N.B., Italy) in distilled water at a frequency of 50 kHz for 22 min.

Immobilization of ZnO nanoparticles

To prepare the ZnO films, dry methods were used [10, 11]. After the pre-treatment, the Zn electrode was weighted, immersed in the colloidal solution and dried in an oven (Dyna, Iran) at 35°C for 30 min. The coated particles were then calcined in a muffle furnace (Shoele, Iran) at 105 and 320°C for 60 min.

Batch EPC reactor

The batch reactor was a 250-ml glass vessel (10×5×5 cm) (Figure 1). The characteristics of the electrodes were as follows: two electrodes of a thin layer of ZnO nanoparticles were immobilized on a Zn (anode) and a copper electrode (cathode). The area of each electrode was 40 cm^2 (10×4×0.1 cm). The distance between the LED UV-A lamp and the Zn/ZnO electrode was adjusted to 2 cm. The alternating current (AC) electrical source (Iran Jahesh, Iran) was equal to 1-5 A. The LED UV-A lamp (OSRAM, Holand) had a radiation intensity of 120 mW cm^{-2}, a wavelength of 395 nm and a voltage of 3.4 V. To evaluate the effect of the current densities, catalyst and UV light on the degradation process, samples underwent LED UV-A lamp treatment at (120, 240, and 360 mW cm^{-2}), with an electrode and thin layer of ZnO nanoparticles immobilized on Zn of (1.5, 3, and 4.5 mg cm^{-2}) at different current densities (3, 6, and 9 mA cm^{-2}), different pHs (4, 7, and 10) and different radiation times (15, 30, and 45 min.).

Analytical methods

All tests were performed in triplicate and the mean data values were reported. The water samples were tested for AR 18, oxidation reduction potential (ORP), pH and temperature by EPC using a spectrophotometer (Hack, America), ORP-meter (CG, Malesia), pH-meter (Hack, America), respectively. The percentage of AR 18 removal was calculated in accordance with the following equation [12]:

$$R(\%) = \left[1 - (Ct / C0\right] \times 100 \qquad (1)$$

where R was the percentage of AR 18 removed, C_{t0} and C_t were the average of AR 18 concentrations in milligrams per before and after treatment.

The kinetics reaction models were determined from the following Equations (2) and (3):

$$\ln Ct = \ln Ct0 - K1t \qquad (2)$$

$$1/Ct = K2t + 1/Ct0 \qquad (3)$$

where C_0 and C_t are the concentrations of AR 18 in the beginning and after a time (t) of the reaction, respectively. K_1 and K_2 were the first and second order reaction constants, respectively [13].

Preparation of water sample

AR 18-contaminated water samples used for EPC experiments were obtained from an urbane distribution system situated at the site of a laboratory in the Islamic Azad University Tehran Medical Sciences Branch in the city of Tehran. The AR 18 was measured by a standard method 2120 C at a wavelength of 510 nm [14]. After each round of the study, reactor water was picked and analyzed to evaluate the efficiency of the removal process. EPC experiments were duplicated and all samples were analyzed in triplicate.

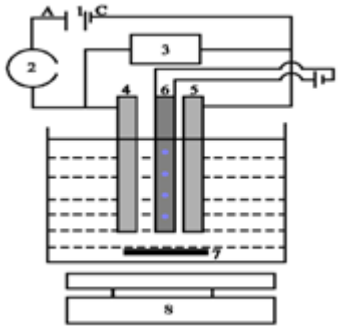

Fig. 1. The batch EPC reactor with a thin layer of ZnO nanoparticles immobilized on Zn (1.Power supply; 2.Current volume; 3.Voltage volume; 4.Copper electrode; 5. Zinc/Zinc oxide electrode; 6. Light emitted dynode ultraviolet-A lamp; 7. Magnetic stirrer bar; 8. Magnetic stirrer

RESULTS AND DISCUSSION

The effect of the initial concentration of AR 18 on the removal efficiency of the EPC process was investigated (Figure 2). The removal efficiency was decreased by an increase in the concentration from 100 to 300 mg L^{-1}. The EPC reactor showed that the removal percentage for an AR 18 concentration (100 mg L^{-1}) decreased from 100% to 82% as the pH increased from 4 to 10, with 15 min. irradiation. The EPC reactor showed the removal percentage for an AR 18 concentration (300 mg L^{-1}) decreased from 82% to 62% as the pH increased from 4 to 10, with 15 min. irradiation. This effect was attributed to increasing the concentration of AR 18 and accordingly fixed the number of photocatalytic sites and UV-A light due to an increase of the adsorbed AR 18 molecules on the catalyst surface. Therefore, fewer photons reached the catalyst surface and the production of $OH^{\cdot}$ radicals decreased because the photocatalytic sites were occupied by AR 18 molecules. The Rate of degradation was decreased. The higher AR 18 concentration played an important role for the inhabitation of $OH^{\cdot}$ radicals during production. Alizadeh *et al.* (2013) investigated the effect of electrocoagulation degradation on the dye reactive orange 16. These experiments were performed at an initial dye reactive orange 16 concentration in the range of 50 to 250 mg L^{-1} at a reaction time of 5 min., a current density of 20 mA cm^{-2} and the removal percentage for dye reactive orange 16 decreased to 10% as the concentration increased from 50 to 250 mg L^{-1} [15]. Abdelwahaba *et al*. (2009) investigated the effect of electrocoagulation degradation on phenol. These experiments were performed at an initial phenol concentration in the range of 0 to 300 mg L^{-1} at pH 7, a reaction time of 120 minute, a distance between the aluminum electrodes of 2 cm and a current density 19.3 mA cm^{-2} [16]. At higher concentrations, the efficiency began to decrease. The EPC reactor reached the highest efficiency (100%) at pH 4, a radiation time of 15 minutes and a concentration of 100 mg L^{-1}. The photocatalytic exposure times required for complete degradation (100 and 200 mg L^{-1}) were 15 and 30 min. This finding was in agreement with previously published data. Saggioro *et al.* (2011) performed an initial study with a C.I Reactive Black R 5 concentration in the range of 30 to 150 mg L^{-1} at acidic pH, TiO_2 0.1g L^{-1}, an irradiation time of 120 min. and a radiation intensity of 260 mW cm^{-2} [17]. At lower concentrations, the photocatalytic exposure time required for complete AR 18 degradation began to decrease. Meena *et al.* (2013) indicated that Methylene Blue immobilized resin Dowex-11 (MBIRD) photocatalyst nanoparticles degraded 40 mg L^{-1} of AR 18 in 160 minutes [18].

The degradation effect of this method was strongly dependent on pH and was enhanced by a decrease in pH. In the EPC process, different concentrations of $OH^{\cdot}$ radicals from water were formed depending on the pH. These products played an important role in the removal of AR 18 concentrations in the EPC process. This effect was attributed to an increase in the availability of OH^{-} anions at an acidic pH that generated more $OH^{\cdot}$ radicals due to decreasing ORP. Basiri *et al*. (2014) investigated the effect of ozone-electrolysis degradation on Azo dye CI AR 18 and informed that the optimum pH was 2 [19]. The decrease in AR 18 removal at pH 10 could be attributed to increasing the oxidation of hydroxide anions in the anode. The optimum pH for reaching the AR 18 standard was 4. The above increased mineralization activity was explained by a higher formation of ROS in the reactor due to accelerating the mass transfer by electron migration of the AR 18 towards the electrode. This effect was also attributed to a decrease in the reduction potential of the reactor at an acidic pH that generated more $OH^{\cdot}$ radicals. The initial and final pH values were measured in this study in order to investigate the effect of pH more effectively. The initial pH was enhanced during EPC studies (Figure 2-3). The EPC reactor reached the highest efficiency (100%) at pH 4, radiation time 15 minutes, ZnO nanoparticles 3 mg/cm^2, distance between the LED UV-A lamp and Zn/ZnO electrodes 2 cm, LED UV-A lamp intensity 360 mW cm^{-2}, current density 3 mA cm^{-2} and an AR 18 concentration of 100 mg L^{-1}. pH 4 requires a lower current density, compared with the two other current densities. The point zero charge point (zpc) of the ZnO was at pH 9.05. The excess positive charge at the ZnO surface, developed the power interaction of the dye with the SO_3^- groups in acidic conditions ($pH \leq pH_{ZPC}$). The SO_3^- groups at AR 18 can gain or lose protons depending on the pH of the sample. Mahanpoor *et al.* (2008) reported using TiO_2 supported on clinoptilolite as a catalyst [20].

The removal percentage for an AR 18 concentration (300 mg L^{-1}) increased from 12% to 15% as the LED UV-A lamp intensity increased from 120 to 360 mW cm^{-2}, with 45 min. of radiation and at pH 4 (Figure 4). The removal efficiency of AR 18 was proportional to the LED UV-A lamp intensity and enhanced by an increase in the LED UV-A lamp intensity since the grater the number of photons produced, required more electrons to migrate from the valence band to the conduction band of the photocatalyst. Kundua *et al.*

(2009) reported the concentration 50 mg L^{-1} of 2,4-dichlorophenoxyacetic acid (2,4-D) decreased progressively from 49.5 mg L^{-1} to 30 mg L^{-1} as the UV-C lamp power increased from 100 to 400 W [21]. At a higher lamp intensity, the exposure time and current density start to decrease. The above increase in optical activity was explained by a higher formation of reactive oxygen species (ROS), such as electron donor $OH^{\cdot}$ radicals from hydroxide anions of water and superoxide anion ($O2^{\cdot -}$) radicals. This phenomenon was attributed to the efficient separation of photo generated holes and electrons, reducing their recombination by the application of an external electric bias. Consequently, more holes were available for the degradation of AR 18 and its intermediates; the photocatalytic process in the EPC process was more effective than the photoelectrochemical (PEC) process alone. This finding was consistent with photocatalytic experiments performed using Ti/TiO_2 nanoparticle electrodes [22]. The removal rate at the same reaction time during the EPC process was larger than the sum of for the PEC and electrochemical (EC) process. Therefore, a synergetic effect was proved, which is consistent with the result in Figure 4. The trend of a linear increase in the degradation rate for AR 18 at given UV-A lamp intensity was explained by producing more electron/hole pairs due to the availability of more photons for excitation at the Zn/ZnO surface.

The removal percentage for AR 18 concentrations dramatically increased in the presence of ZnO photocatalyst nanoparticles and the LED UV-A lamp since the availability of a greater catalyst surface area for absorption of photons and the interaction of AR 18 reaction with the ZnO catalyst led to an increase in the number of holes and $OH^{\bullet}$ radicals generated (Figure 5). At a higher lamp intensity along with a higher amount of ZnO catalyst, up to 3 mg cm^{-2}, the exposure time, and current density start to decrease. At fixed lamp intensity, it was that an optimum catalyst amount would present where the photocatalyst would form a maximum concentration of ROS which could take part in a reaction at the outer film surface. The optimum amount of ZnO catalyst had the highest surface for decay of AR 18. The optimum amount of ZnO catalyst concentration and optimum intensity of the LED UV-A lamp reaching the AR 18 standard were 3 mg cm^{-2} and 360 mW cm^{-2}, respectively. While the removal efficiency decreased at 1.5 and 4.5 mg cm^{-2} of ZnO nanoparticle films, it reached the highest value (100%) for 3 mg cm^{-2} ZnO nanoparticle film. This finding was attributed to an increase in the surface area for degradation of AR 18 concentrations. Elaziouti *et al.* (2011) concluded that the decay rate constant of Congo red (CR) was proportional to the ZnO concentration. The decay rate enhanced from 68.73 to 90.02% as the ZnO concentration was increased from 0.25 to 0.5 g/L. However, the increase in the ZnO concentration more than 0.5 g/L led to a decrease in the decay rate of CR [23]. However, a limiting value was observed for thick films due to an increase in opacity and light scattering leading to a decrease in the passage of irradiation through the film. At higher catalyst loadings (i.e. more than 3 mg cm^{-2}) the removal efficiency of AR 18 started to decrease due to the photo emission. This phenomenon was attributed to a decrease in UV penetration through the outer layers of the film and a decrease in protection due to the clusters blocking UV from reaching the catalyst surface. The presence of ZnO photocatalyst nanoparticles and UV-A led to increasing the removal efficiency of AR 18 and generation of $OH^{\bullet}$ radicals. Nafie and Yasmen (2013) used ZnO and UV-A LED for degradation of phenol [24]. $OH^{\bullet}$ radicals led to oxidation of AR 18. The $O2^{\bullet -}$ hydro peroxyl radical and hydrogen peroxide generated by the reduction of dissolved oxygen in the anode, could also feed the photocatalytic degradation mechanism. These species were responsible for degrading the AR 18. Madhusudhana *et al.* (2012) reported the photocatalytic degradation of the Violet GL2B azo dye using CaO and TiO_2 nanoparticles [25].

A key variable parameter affecting the oxidation ability of EPC processes was the applied current density since it regulated the amounts of generated $OH^{\bullet}$ radicals acting as oxidizing agents. At a lower current density and a lower radiation time the removal efficiency of AR 18 began to decrease (Figure 6). The optimum current density for AR 18 as a standard is 9 mA cm^{-2}. At lower initial concentration loadings, the photocatalytic treatment time required for complete degradation started to decrease. The experimental results show that the current density electrode enhances the resulting gradient separated electron–holes, thereby diminishing its recombination rate, enhancing the photocurrent rate and expediting the degradation as shown in Figure 3. Under higher applied current densities, the external electric field improved the direct and indirect electro-oxidation reactions at the anode. The degradation efficiency was proportional to the specific surface area of photocatalysts because the number of $OH^{\bullet}$ was proportional to the specific surface area and inversely proportional to the electron-hole recombination rate. The

photoelectrocatalytic process accelerated the mass transfer by electro-migration of AR 18 towards the electrode. The selection of current densities is dependant on the removal efficiency of AR 18 and the cost of the consumed electrical energy. This finding is in unison with the photocatalytic experiments carried out using graphite-supported TiO_2 by Maljaei *et al.* (2009) [26]. The experimental results showed that the more intense the radiation penetrating the photocatalytic electrode, the faster the AR 18 degradation progressed. As expected, the current density and exposure time were enhanced accordingly the removal efficiency of AR 18 was increased as shown in Figure 3. This finding was the same as for the UVA photoelectro-Fenton degradation experiments carried out using the BDD reactor by El-Ghenymy *et al*. (2013) [27]. The increase in current density and exposure time led to faster generation of electrolysis products such as OH^- anions at the cathode electrode. This product was responsible for AR 18 degradation. Increased current density led to an increased drift force on the electrode surface, which was the main factor in the electrochemical processes. These finding are the same as the experiments performed using the electrode by Isarain-Chávez *et al.* (2010) [28]. The oxygen produced on the anode electrode led to the effect of higher degradation of AR 18, because the oxygen molecules play an important role at the stage of photocatalysis and transformed to $O2^{\bullet-}$ radicals bound to the ZnO photocatalyst nanoparticles. This finding was the same as shown by the photocatalytic experiments performed using ZnO by Sushil *et al*. (2009) [29]. At a current density of more than 20 mA cm^{-2}, the removal efficiency started to decrease at higher temperatures in the reactor due to the disintegration of the $OH^{\bullet}$ radicals. Farhadi and Aminzadeh (2012) showed that the COD removal efficiency was increased to 32% at 1.83 mA cm^{-2} from 12% at 0.43 mA cm^{-2} after 30 min. of reaction time [30].

The pattern of the EPC decay mechanism for AR 18 was distinguished by the complex structure of the -N=N- and SO_3^- groups. The negative charge of the AR 18 led to its absorption by the Zn/ZnO electrode and could be mineralized, eroded by strong oxidants such as positive holes and $OH^{\bullet}$ radicals or reduced by electrons. The increase in current density and exposure time led to faster generation of electrolysis products such as OH^- and Cl^- anions at the cathode and anode electrodes, respectively. These products were responsible for AR 18 inactivation. Increased current density led to an increased drift force on the electrode surface, which was the main factor in electrochemical processes. Therefore, it is obvious that the generation of an adequate quantity of reactive oxygen species for the oxidation of AR 18 requires the optimum radiation time (30 min). This finding was the same as for the experiments performed using an N-doped TiO_2 photoanode by Daghrir *et al.* (2014) [31]. Clearly, the band gap of the ZnO semiconductor (Eg = 3.2 eV) is close to that of the UV-A radiation LED lamp (E_{UV-A} =3.4 eV). The photogenerated electron (e^-)-hole (h^+) pairs could be facilely isolated and transferred to the semiconductor/adsorbate interface efficiently, therefore enhancing the photocatalytic activity. This finding is the same as the photocatalytic experiments carried out using a UV light by Tomasevic *et al*. (2009) [32]. The oxygen produced at the anode electrode led to a higher degradable effect of AR 18, because oxygen molecules play an important role at the photocatalysis stage and transformed to $O_2^{\bullet-}$ radicals as bonds in ZnO photocatalyst nanoparticles. These findings are the same as the photocatalytic experiments performed using TiO_2 by Pelaez *et al.* (2012) [33]. The efficiency of AR 18 absorption by a Zn electrode covered by a layer of ZnO nanoparticles as a positive pole (anode) is directly related to an increase in current density and exposure time. This electrophotocatalytic mechanism is illustrated by the following equations:

$$ZnO + h\nu\ (\lambda = 390\ nm) \dashrightarrow ZnO\ (e^-_{(CB)} + h^+_{(VB)}) \quad (6)$$

$$O_2 + H_2O \dashrightarrow O_3 + 2H^+ + 2e^- \quad (7)$$

$$e^-_{(CB)}\ (ZnO) + O_{2ads} \dashrightarrow O_{2ads}^{\bullet-} + ZnO \quad (8)$$

$$O_{2ads}^{\bullet-} + H^+ \dashrightarrow HO_{2ads}^{\bullet-} \quad (9)$$

$$HO_{2ads}^{\bullet-} \dashrightarrow O_2 + H_2O_2 \quad (10)$$

$$H_2O_2 + h\nu \dashrightarrow 2\ OH^{\bullet} \quad (11)$$

$$h^+_{(VB)} + OH^- \dashrightarrow OH^{\bullet} \quad (12)$$

$$\bullet OH + AR\ 18 \rightarrow \text{degradation of the AR 18} \quad (13)$$

The results of the AR removal efficiency by the Taguchi model showed that the concentration was the most important variable (Figure 7). This finding was not consistent with the experiments performed using iron electrodes by Chandra *et al*. (2011) [34]. It was concluded that the influence of the initial pH of the solution on the photocatalysis kinetics was due to the amount of the dye adsorbed on ZnO. On the other hand the reaction developed the ZnO surface near the surface catalyst and not in the solution. This finding was consistent with the experiments performed using hydroxide/TiO_2 nanoparticles by Wang *et al*. (2008) [35].

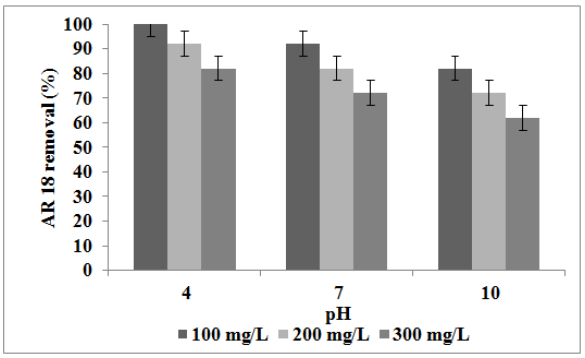

Fig. 2. Effect of the initial AR 18 concentration and pH on the efficiency of AR 18 removal (pH 4-10; Temperature 25°C; Radiation time 15 min; UV-A lamp intensity 360 mw cm^{-2}; Initial AR 18 concentration 100-300 mg L^{-1}; Current density 3 mA cm^{-2}; Zinc oxide concentration 3 mg L^{-1}).

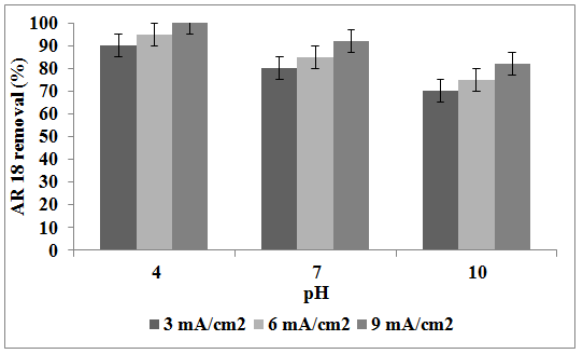

Fig. 3. Effect of the pH on the efficiency of AR 18 removal (pH 4-10; Temperature 25°C; Radiation time 30 min; UV-A lamp intensity 360 mw cm^{-2}; Initial AR concentration 300 mg L^{-1}; Zinc oxide concentration 3 mg L^{-1}).

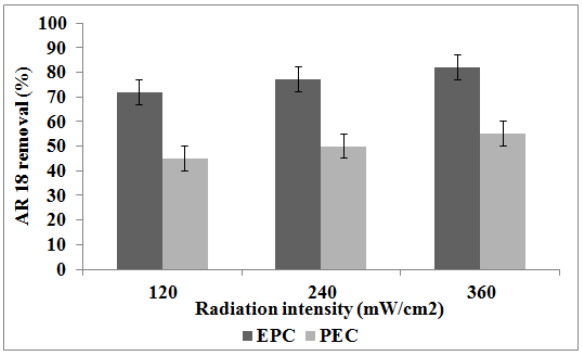

Fig. 4. Effect of the UV radiation and catalyst on the efficiency of AR 18 removal (pH 4; Temperature 25°C; Radiation time 15 min.; UV-A lamp intensity 120-360 mw cm^{-2}; Initial AR 18 concentration 300 mg L^{-1}; current density 3 mA cm^{-2}).

The experimental data are a better fit to the first order reaction (Figure 8). The regression coefficient for the fitted line was calculated to be $R^2 = 0.9898$ for AR 18. The apparent rate constant, K_1 and the half-life time, $t_{1/2}$ were calculated to be 0.013 min^{-1} and 0.7 min. Mohammadlou *et al.* (2014) concluded that the electrocoagulation degradation of the CR follows first-order kinetics [36]

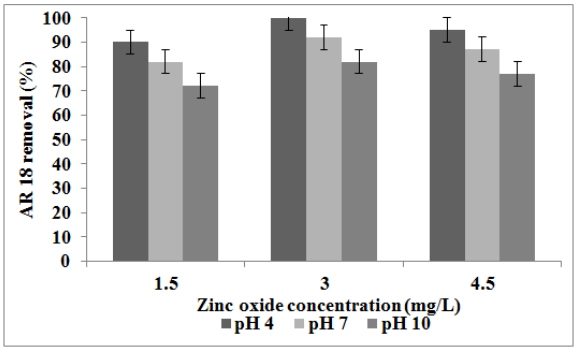

Fig. 5. Effect of the catalyst layer on the efficiency of AR 18 removal (pH 4-10; Temperature 25°C; Radiation time 15 min; UV-A lamp intensity 360 mw cm^{-2}; Initial AR 18 concentration 300 mg L^{-1}; current density 3 mA cm^{-2}.

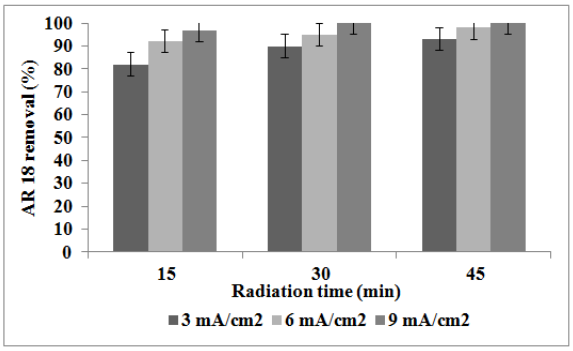

Fig. 6. Effect of the current density on the efficiency of AR 18 removal (pH 4; Temperature 25°C; Radiation time 15-45 min; UV-A lamp intensity 360 mw cm^{-2}; Initial AR 18 concentration 300 mg L^{-1}; current density 3-9 mA cm^{-2}; Zinc oxide concentration 3 mg L^{-1}).

CONCLUSION

The experimental results show that the batch EPC reactor is a practical and promising method in AR 18-contaminated water. The EPC reactor is more effective than the PEC reactor. AR 18 degradation is affected by the pH, the concentration of AR 18, the concentration of ZnO nanoparticles, the radiation time and current density. The EPC is capable of AR 18 removal at the pH value (4) investigated with a radiation time less than 15 min. Enhanced AR 18 removal is obtained with an increase in the radiation time and current density. It is purposed that the performance of process is studied the other electrode material.

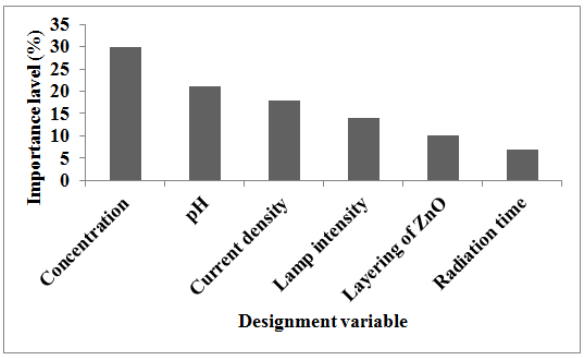

Fig. 7. The Taguchi model.

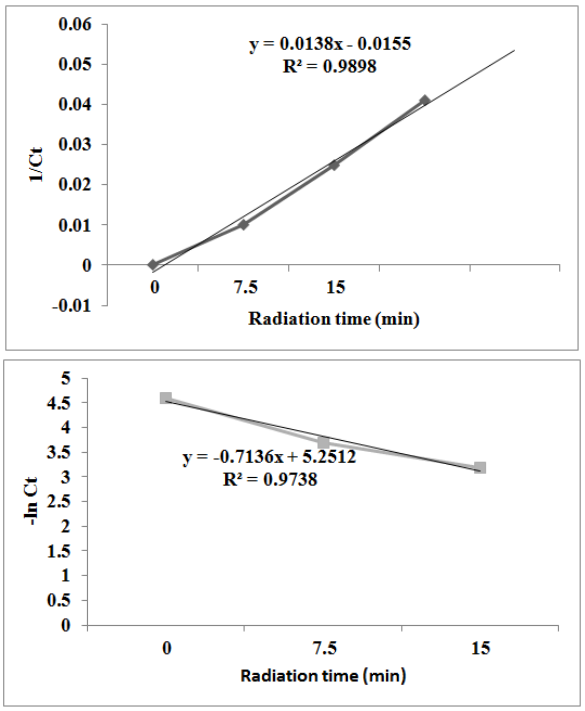

Fig. 8. The plots of first and second order reaction models fitted with the AR 18 removal experimental data in the batch EPC reactor (experimental conditions: 25 ºC, pH: 7, reaction time: 0-15 min).

Acknowledgements: *The author thanked the Department Environmental Health of Islamic Azad University, Tehran Medical Sciences Branch for financial and instrumental supports.*

REFERENCES

1. M. Mukhlish, B. Zobayer, M.M. Huq, M.S.I. Mazumder, M.R. Khan, M.A. Islam, *Int. Res. J. Environ. Sci.*, **2** (6), 49 (2013).
2. A. Maleki, A.H. Mahvi, R. Ebrahimi, Y. Zandsalimi, *J. Chem. Engin*., **27**, 79 (2010).
3. I. Maghri, A. Kenz , M. Elkouali , O. Tanane, M. Talbi, *J. Mater. Environ. Sci.*, **3**, 121 (2012).
4. G.R.D. Oliveira, N.S. Fernandes, J.V.D. Melo, D.R.D. Silva, C. Urgeghe, C.A. Martı´nez- Huitle, *Chem. Engin. J.*, **168**, 208 (2011).
5. D. Arsene, C. Petronela Musteret, C. Catrinescu, P. Apopei, G. Brajoveanu, C. Teodosiu, *J. Environ. Engin. Manag.*, **10**, 1967 (2011).
6. C. Ratiu, F. Manea, C. Lazau, I. Grozescu, C. Radovan, J. Schoonman, *Desalin.*, **260**, 51 (2010).
7. I. Sirés, E. Brillas, Env. Int., **40**, 212 (2012).
8. J. Georgieva, E. Valova, S. Armyanov, N. Philippidis, I. Poulios, S. Sotiropoulos, *J. Hazard. Mater.*, **211**, 30 (2012).
9. S. Guy, P. Yaron, Int. J. Photoenergy., Article ID 596710, 1-7 (2011).
10. S. Malato, P. Fermandez-Ibanez, M.I. Maldonado, J. Blanco, W. GernJak, *J. Catal. Today*., **147**, 1 (2009).
11. C. Zuolian, T. Kok-Eng, T. Yong, G. Amos, Y. Xi-Jiang, *Sustain. Environ. Res.*, **20**, 281 (2010).
12. D. Hua, K. Cheuk, Z. Wei-ning, W. Chen, X. Chang-Fa, *J. Trans. Nanoferrous Met. Soc. China.*, **17**, 700 (2007).
13. A.O. Ifelebuegu, T.J. Mason, J. Eadaion, J. Onubogu, *Int. J. Environ. Sci. Technol*., **11,** 1 (2014).
14. APHA: Standard methods for the examination of water and wastewater. 22st Edn. APHA, AWWA, WPCF, Washington DC, USA (2012).
15. M. Alizadeh, A.H. Mahvi, H. Jafari Mansoorian, R. Ardani, *Iranian J. Health, Safety & Environ.*, **1** (1), 1 (2013).
16. O. Abdelwahaba, N.K. Aminb, E-S.Z. El-Ashtoukhyb, *J. Hazard. Mater*., **163**, 711 (2009).
17. E.M. Saggioro, A.S. Oliveira, T. Pavesi, C. G. Maia, L.F. Vieira Ferreira, J.C. Moreira, *Molecules*., **16**, 10370 (2011).
18. R.C. Meena, S. VermaHimakshi, S. Disha, *Int. Res. J. Environ. Sci.*, **2** (12), 35 (2013).
19. J. Basiri Parsa, M. Golmirzaei, M. Abbasi, J. *Industrial Engin. Chem*., **20**, 689 (2014).
20. K. Mahanpoor, K. Gholivand, M. Nikazar, *J. Desalin*., **219**, 293 (2008).
21. S, Kundua, A. Pala, A.K. Dikshit: UV induced degradation of herbicide 2,4-D: kinetics, mechanism and effect of various conditions on the degradation.
22. N. Philippidis, S. Sotiropoulos, A. Efstathiou, I. Poulios, *J. Photochem. Photobiol. A: Chem.*, **204**, 129 (2009).
23. E. Elaziouti, N. Laouedj, B. Ahmed, *J. Chem. Engin. Process Technol.*, **2 (**2), 1 (2011).
24. A.A. Nafie, H.Z. Yasmen, Global Res. Analtsis., 2 (1), 2013.
25. N. Madhusudhana, K. Yogendra, K.M. Mahadevan, *Int. J. Engin. Res. Applications.*, **2** (5), 1300 (2012).
26. A. Maljaei, M. Arami, N.M. Mahmoodi, *Desalin.*, **249**, 1074 (2009).
27. A. El-Ghenymy, N. Oturan, M. A. Oturan, J.A. Garrido, P.L. Cabot, F. Centellas, R.M. Rodríguez, E. Brillas, *Chem. Engin, J.*, **234**, 115 (2013).
28. E. Isarain-Chávez, C. Arias, P.L. Cabot, F. Centellas, R.M. Rodríguez, J.A. Garrido, E. Brillas, *Appl. Catal. B: Environ*., **96**, 361 (2010).
29. K. Sushil, N.K. Kansal, S. Sukhmehar, *Nanoscale Res. Letter*, **4**., 709 (2009).
30. S. Farhadi, B. Aminzadeh, *J. hazard. Mater*., **35**, 219 (2012).

31. R. Daghrir, P. Drogui, N. Delegan, M.A. El-Khakani, *Sci. Total Environ*., **466-467**, 300 (2014).
32. A. Tomasevic, J. Đaja, S., Petrovic, E.E. Kiss, D. Mijina, *Chem. Industry Chem. Engin. Quarterly.,* **15**, 17 (2009).
33. M. Pelaez, N.T. Nolan, S.C. Pillai, *Appl. Catal. B-Environ.,* **125,** 331 (2012).
34. S.V. Chandra, D. Patil, S.K. Kumar, *Int. J. Chem. Reactor Engin.,* **9** (1), 1 (2011).
35. N. Wang, J. Li, L. Zhu, Y. Dong, H. Tang, *J. Photochem. Photobiol. A Chem*., **198**, 282 (2008).
36. N. Mohammadlou, M.S. Rasoulifard, M. Vahedpour, M.R. Eskandarian, *J. Appl. Chem.Res.*, **8** (4), 123 (2014).